



**HAL**  
open science

# MicroPress: Detecting Pressure and Hover Distance in Thumb-to-Finger Interactions

Rhett Dobinson, Marc Teyssier, Jürgen Steimle, Bruno Fruchard

► **To cite this version:**

Rhett Dobinson, Marc Teyssier, Jürgen Steimle, Bruno Fruchard. MicroPress: Detecting Pressure and Hover Distance in Thumb-to-Finger Interactions. Proceedings of the 2022 ACM Symposium on Spatial User Interaction (SUI 2022), Dec 2022, Online CA USA, France. pp.1-10, 10.1145/3565970.3567698 . hal-03850971

**HAL Id: hal-03850971**

**<https://hal.science/hal-03850971v1>**

Submitted on 14 Nov 2022

**HAL** is a multi-disciplinary open access archive for the deposit and dissemination of scientific research documents, whether they are published or not. The documents may come from teaching and research institutions in France or abroad, or from public or private research centers.

L'archive ouverte pluridisciplinaire **HAL**, est destinée au dépôt et à la diffusion de documents scientifiques de niveau recherche, publiés ou non, émanant des établissements d'enseignement et de recherche français ou étrangers, des laboratoires publics ou privés.

# MicroPress: Detecting Pressure and Hover Distance in Thumb-to-Finger Interactions

Rhett Dobinson

rhett Dobinson@gmail.com

Saarland University, Saarland Informatics Campus  
Germany

Jürgen Steimle

steimle@cs.uni-saarland.de

Saarland University, Saarland Informatics Campus  
Germany

Marc Teyssier

marc.teyssier@devinci.fr

Research Center, Léonard de Vinci Pôle Universitaire  
France

Bruno Fruchard

bruno.fruchard@inria.fr

Univ. Lille, Inria, CNRS, Centrale Lille, UMR 9189 CRISTAL  
France

## ABSTRACT

Thumb-to-finger interactions leverage the thumb for precise, eyes-free input with high sensory bandwidth. While previous research explored gestures based on touch contact and finger movement on the skin, interactions leveraging depth such as pressure and hovering input are still underinvestigated. We present MicroPress, a proof-of-concept device that can detect both, precise thumb pressure applied on the skin and hover distance between the thumb and the index finger. We rely on a wearable IMU sensor array and a bi-directional RNN deep learning approach to enable fine-grained control while preserving the natural tactile feedback and touch of the skin. We demonstrate MicroPress' efficacy with two interactive scenarios that pose challenges for real-time input and we validate its design with a study involving eight participants. With short per-user calibration steps, MicroPress is capable of predicting hover distance with 0.57mm accuracy, and on-skin pressure with 6.71% normalized pressure error at 6 locations on the index finger.

## CCS CONCEPTS

• **Computing methodologies** → **Neural networks**; • **Human-centered computing** → **Interaction devices**.

## KEYWORDS

Thumb-to-Finger Interaction, Gestural Input, Hover Input, Pressure Input, Deep Learning, IMU, RNN, LSTM

### ACM Reference Format:

Rhett Dobinson, Marc Teyssier, Jürgen Steimle, and Bruno Fruchard. 2022. MicroPress: Detecting Pressure and Hover Distance in Thumb-to-Finger Interactions. In *Symposium on Spatial User Interaction (SUI '22)*, December 1–2, 2022, Online, CA, USA. ACM, New York, NY, USA, 10 pages. <https://doi.org/10.1145/3565970.3567698>

## 1 INTRODUCTION

Directly interacting on the skin has generated a lot of interest in HCI in the past decade [44]. Skin interactions offer "device-free"

and intuitive gestures [14, 27, 54, 55]; the deformable surface of skin furthermore allows for expressive gestural interaction [2, 47]. In this context, thumb-to-finger interactions [41] are particularly interesting, as they are shown to be private, precise [6, 51] and comfortable [17]. They can offer high accuracy in eyes-free conditions with minimal training; moreover, using the thumb for gesturing on the skin preserves the natural haptic feedback of human touch [17, 21].

To date, work in the area of thumb-to-finger interactions mostly focused on touch contact interactions, thus only partly leveraging the potential of interacting on the skin. The most comprehensive design space for such interactions proposed by Soliman et al. [41] considered four dimensions: the touch initiator (thumb or index fingers), the touch location on the finger, the gesture performed, and the flexion of the fingers while interacting. We propose to add the depth dimension to this design space by enabling pressure and hovering input for thumb-to-finger interactions (Figure 1a). Depth enables more input capacity at all touch locations using the thumb, and introduces hovering movements that extend the breadth of interactions before or after skin contact. Such interactions promise to enhance the expressiveness of gestures and require minimal movement of the fingers, promoting social acceptability when interacting with smart-glasses or smartwatches.

The primary challenge in recognizing such subtle interactions is the level of precision required by users to fully control an interactive system while maintaining natural touch and skin feedback. A wide variety of technologies have been proposed to detect microgestures and thumb-to-finger gestures, such as millimeter wave radar [27], inertial measurement units (IMUs) [43], optical cameras [41], capacitive on-skin devices [51], or magnetic field sensors [17]. While sensing techniques relying on computer vision are prone to occlusion, IMUs and magnetic field sensors are not. We used the magnetic sensitivity of the IMU by placing a magnet on the thumb nail to sense movements [30]. Although this requires sensors and magnets to be worn on the hand, they typically do not impede comfort or natural hand movement. Combined with deep learning techniques, these sensors can enable fine-grained gesture recognition and motion capture. For instance, recurrent neural networks (RNN) with Long Short-Term Memory architecture (LSTM) have been successful for estimating human pose [18] and recognizing thumb-to-finger microgestures [46].

*SUI '22, December 1–2, 2022, Online, CA, USA*

© 2022 Association for Computing Machinery.

This is the author's version of the work. It is posted here for your personal use. Not for redistribution. The definitive Version of Record was published in *Symposium on Spatial User Interaction (SUI '22)*, December 1–2, 2022, Online, CA, USA, <https://doi.org/10.1145/3565970.3567698>.



**Figure 1: a) MicroPress leverages depth for thumb-to-finger interactions by enabling real-time hover and pressure input. b) It relies on IMU sensors placed on the index finger's, and a magnet placed on the thumb.**

We contribute MicroPress, a proof-of-concept system that can detect pressure applied with the thumb at different locations on the index finger, and the hovering distance between the thumb fingertip and the index finger in real-time (Figure 1b). This system's goal is to demonstrate the benefits and capabilities of the interaction technique through application example. Our implementation preserves the natural hand movement and sensory feedback of the skin by relying on Inertial Measurement Unit (IMU) sensors placed on the three phalanges of the index finger, a small magnet placed on the thumbnail, and deep learning leveraging Bi-directional LSTM RNNs for times series data processing. We trained two deep learning models that work together: the first infers pressure and location, while the second infers distance. We show MicroPress' efficacy through two interactive applications that pose challenges for real-time input: selecting commands in linear menus and controlling the movements of a video game character in 2D. We evaluate its design through a validation study involving eight participants, following well-established pressure input tasks [12, 42]. To the best of our knowledge, MicroPress is the first system to date to demonstrate the possibility to recognize pressure and hovering input for thumb-to-finger interactions.

## 2 RELATED WORK

We review related work on thumb-to-finger interactions and discuss the numerous sensing technologies and their potential in detecting pressure and hover distance. We relate these to the existing thumb-to-finger interaction design space, highlighting the potential to expand this space using the depth dimension.

### 2.1 Thumb-to-finger Interactions

The human hand is a highly dexterous structure that provides significant performance advantages over other muscle groups of the human body [53]. Fingers allow for accurate and fluid gestures [27, 41, 51] and provide means for private, subtle [6, 51] and eyes-free interactions [17, 21]. This precision is largely due to the natural tactile feedback and proprioceptive qualities of moving and touching fingers [49]. The thumb is also highly dexterous and can be used to point at various locations on the fingers in a comfortable way [17].

Touch and microgestures have been the focus of previous work in thumb-to-finger interactions. Earlier work focused mostly on touch and stroke interactions. The design space developed by Soliman et al. [41] consists of four primary dimensions: the touch initiator

(finger or thumb), the finger segment where the interaction happens, a gesture action (tapping, sliding along or around the fingers), drawing a shape, and the fingers flexion. While some devices enable pressure input [49], no device primarily focus on sensing depth. Yet, doing so enables to detect precisely when a user touches their skin and expands the interactions capacity before and after touch contact. MicroPress demonstrates how to sense depth in the context of thumb-to-finger interactions.

### 2.2 Pressure and Hovering Input

The literature demonstrated the high input bandwidth of pressure input in various contexts such as pen input [38], mouse input [4], back-of-device interactions [10], cloth interaction [42], or while interacting on deformable surfaces [12]. These studies focused on evaluating user performance through visual targeting tasks and showed high accuracy rate for  $10 \pm 2$  discrete levels [4, 38, 40, 42, 50]. Fruchard et al. [12] recently reported higher input bandwidth with soft surfaces, achieving a 5% error rate for 20 discrete levels, hinting that the potential for pressure input may have been underestimated. In the context of thumb-to-finger interactions, pressure input is an ideal mode of interaction, requiring minimal movement and small, fingertip-sized interactive areas. We investigate such interactions with MicroPress and evaluate its accuracy with a dwelling mechanism (cf. [11, 38]) to validate its design.

Detecting hovering distance on capacitive touch surfaces enables additional controls compared to touch interactions [9, 15, 45]. Hinckley et al. [15] explored multi-layered interfaces one navigates using the finger distance from a device, improving pointing accuracy by inferring finger trajectory, and providing multi-finger interactions to control the position of menus. Such interactions are also useful for around-device interactions [30] to avoid occluding visual information on display and leverage the space surrounding a device, or for avoiding to mark the touch area with oily smudge patterns in the context of touch-based unlocking patterns [24].

### 2.3 Sensing Thumb-to-Finger Input

Various technologies have been investigated for sensing hand-based interaction. Computer vision using RGB or depth cameras is a commonly used technology [5, 28, 35, 41, 52]. For instance, the user can wear a camera on the shoulder [41], the fingers [5], or the wrist [52]. Computer vision approaches, however, are susceptible to occlusion problems and suffer from a limited field of view, despite solutions leveraging deep learning techniques [32]. Ishikawa et al. [20] propose to position an array of ranging sensors on the

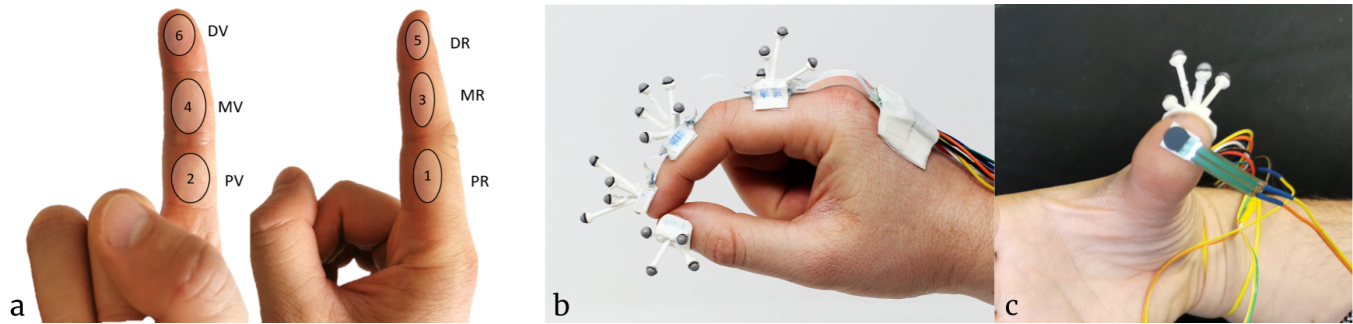


**Figure 2: (a) Zones considered on the index finger. DV, MV, PV correspond to the Distal, Middle and Proximal segments on the Volar side, and DR, MR, PR segments correspond to the Radial side. (b) We mounted 3D printed markers on the magnet and three sensors to precisely capture their positions using an Optitrack system. (c) Placement of the FSR sensor to measure thumb tip to finger pressure.**

wrists for identifying which finger touches and hovers at the back of the hand. Millimeter-wave radars enable accurate fingertip and hand gesture recognition [26, 27], but are typically located on a fixed surface and require the user to interact in front of the sensor. Thin-film capacitive sensors worn on the skin enable touch interactions in various postures, mobility and lighting conditions [34, 48]. Capacitive touch sensing is also used in gloves to detect continuous touch and pressure input [49]. While capacitive surfaces can detect hovering movements, it is unclear what precision they would achieve while bent and attached to the users skin.

Our work leverages inertial measurement units (IMUs) that can detect acceleration and rotational velocity simultaneously. IMU data sensor fusion algorithms allow for accurate measurement of hand pose and orientation [39] and higher-level gesture recognition [22]. IMU sensors are small enough to be easily integrated into wearable devices and ergonomically worn on the fingers [39] or in a ring form factor [43], and do not require line-of-sight. Similarly, magnetic field sensors do not require line-of-sight and can be used for precise positional tracking [1, 6–8, 17, 30, 37]. IMU raw data is however not readily usable. Sensor fusion algorithms are required to create the sensors orientation vector, adding complexity and sources of error. Like most electronic devices, noise is a consideration in data generation, and results in drift and uncertainty in the IMUs data. This can reduce accuracy of measurements as the measured vs actual position of the sensor diverge. We use a data driven deep learning approach to help reduce these effects.

## 2.4 Processing sensor input with deep learning

Deep Learning models have demonstrated their ability in enhancing traditional sensing methods for interaction and gesture recognition. Soli [27] is a millimeter wave radar system that leverages Long Short-Term Memory (LSTM) recurrent neural networks (RNNs) to capture temporal sequence information and classify dynamic microgestures [46]. Soli’s LSTM approach also enables the expansion of the gesture space just by adding new training data, and is 100% accurate in recognising non-gesture inputs, preventing accidental interactions. Lai et al. [23] also leveraged LSTM RNNs in classifying skeleton based hand gestures with 85% accuracy. LSTM networks are demonstrably suitable for sequence based gesture classification,

and are well supported by widely used machine learning frameworks such as Pytorch [36].

Neural networks are not only useful for gesture classification, but can be used in regressing other measurements from IMU sensor data. Deep Inertial Poser (DIP) [18] reconstructs real-time human pose from sparse IMU sensor orientation sequence data using a bi-directional LSTM model. We chose to use the BI-LSTM model because it is able to learn the mapping between times series features, IMU data and kinematic body model parameters, which is the basis of our proof-of-concept. Instead of hand or body pose, we learn the mapping of pressure and precise optical tracking data to small changes in magnetic field and IMU sensor orientation due to pressing the thumb and finger together, and hovering the thumb above the fingers. We demonstrate with MicroPress that Bi-LSTM models using IMU orientation and magnetic field motion sequence data are able to infer pressure, position and distance measurements in real time.

## 3 MICROPRESS: SENSING HARDWARE AND DEEP LEARNING MODELS

The MicroPress system relies on two main elements: a hardware element that consists of an array of 3 IMU sensors on the index finger and a small magnet placed on the thumb, Figure 1b, and a software element composed of an embedded sensor fusion and a machine learning pipeline with 2 models. The primary reasons for choosing IMU sensing was to preserve skin contact between the thumb and fingers, to enable occlusion-free magnetic field sensing and to gather finger segment orientation data through sensor fusion algorithms. The sensors are also readily available, low in cost and easily integrated into electronic circuits.

The IMUs are Bosch BMX160 9-axis IMUs combined with sensor fusion algorithms [3, 16] to generate synchronized acceleration, angular velocity, magnetic field and 4D sensor orientation data as inputs to our models. 9-Axis IMUs provide many data points from a single sensor. The magnet’s magnetic field is much stronger than ordinary ambient fields. When paired with integrated sensitive 3-axis magnetometers in the selected IMUs, it is capable of sensing sub-millimeter motion required for precise depth measurement. We made assumptions that the deep learning model would adapt to

magnetic field interference and the stability of the sensor fusion algorithms given sufficient data in an uncontrolled lab environment.

Similar to IMU arrays used in related work [39], we designed a PCB that can be linked together with flexible cables to form an array attached to the top of the index finger, see Figure 1b. Each IMU is attached with double-sided tape to the back of the finger on each phalanx: distal (tip), middle, and proximal (base). This design keeps the fingertips uncovered to preserve tactile feedback. We interface to the sensor array with a *Teensy 3.2* microcontroller over Serial Peripheral Interface (SPI) bus.

The second hardware component is a small magnet placed on the thumbnail. We informed the magnet location from previous work [6, 17] and selected a radial 6x2.5mm Neodymium-Iron-Boron permanent magnet as the magnetic field source. This particular magnet allows using the magnetometer’s full dynamic range, without reaching saturation when the thumb and index finger are fully pressed together. We divided the area on the index finger into 6 touch zones as shown in Figure 2a, with 2 zones for each of the distal, middle and proximal segments corresponding to the radial and volar sides [41].

Finally, we developed deep learning models that can infer real-time thumb-tip to finger hover distance, and on-skin pressure at each of the 6 discrete touch zones. We differentiate each zone based on the distance from the thumb-tip magnet and each individual IMU. Data from the IMUs is collected through USB serial at 100 Frames Per Second (FPS) which is the maximum output data rate (ODR) of the sensor fusion algorithms. A single processed input frame consists of 39 features; 27 from the 9-axis IMU sensors, and a 4D sensor fusion orientation quaternion from each IMU.

### 3.1 Data Collection

Collecting ground truth data was performed separately for pressure and hover distance to be able to focus on these tasks independently and separate the optimization of the models.

*Pressure and Touch Ground Truths.* We used a 4mm wide Force Sensing Resistor (FSR), designed to support a range of 10Nm which matched earlier work sensing pinch pressure [12, 25]. The FSR was stuck to the tip of the thumb so that the thumb-tip to finger pressure can be measured Figure 2c. The sensor voltage was measured using the 10-bit (0-1023) analog-to-digital converter on the MCU.

To better determine the systems effectiveness at different locations on the finger, the IMU and pressure data were collected in separate sessions for each touch zone. To gather touch data, we used a switch connected to a digital input on the MCU, that the user would press and hold for the duration of touch contact. This effectively labelled the data as touch or no touch, with the touch value corresponding to the zone of that session.

Data was collected from 3 users who randomly varied hand orientation, pressure, finger flexion and speed to help generalize the system to all possible applications. We collected 30 minutes of data from user 1, 5 minutes from user 2 and 10 minutes from user 3. This was repeated for each of the 6 zones, totalling 7 hours and 38 minutes of data or 2.748 million frames at 100 FPS.

*Hover Distance Ground Truths.* To gather distance ground truths, we designed and 3D printed optical tracking markers for each IMU and the thumb magnet using 4mm reflective hemispheres.

Then with an Optitrack motion-capture system, we recorded global XYZ thumb-tip and IMU sensor coordinate, see Figure 2b. The system was calibrated to 0.2mm residual error using 9 cameras in a 70cm square field, allowing us to measure position with sub-millimeter precision. We generated ground truths by calculating the Euclidean distance in meters between the thumb marker and each of the finger marker coordinates, generating three distances per IMU sample. IMU and Optitrack data were synchronized using Optitrack’s Motive Python API to generate inputs and ground truth data.

To capture hover distance ground truths, the user moved the thumb tip relative to each IMU sensor on the finger with the goal of simulating real world hover and distance interactions. We also varied hand orientation, speed and dwelling time at different hover distances to help generalize the data to future applications. We collected 960 000 frames of data over 2 hours and 40 minutes at 100 FPS from a single user.

Overall the samples were recorded from 3 users (2 identified as male, 1 identified as female) aged from 27 to 32 years old (median = 28.7). We measured their finger and thumb dimensions for the distal, middle, and proximal sections. Measurements for the index finger; 22 to 24mm ( $\bar{x} = 23.3$ , distal), 24 to 28mm ( $\bar{x} = 26.7$ , middle), and 42 to 46mm ( $\bar{x} = 44.0$ , proximal) section lengths, and for the thumb; 32 to 34mm ( $\bar{x} = 33.3.0$ , distal) and 31 to 45mm ( $\bar{x} = 38.3$ , proximal).

*Dataset Creation.* We created two separate datasets from the data collection step. We used all available input features for each model, with both datasets having 39 features per input frame. The 27 values from the 3 9-axis IMUs were in LSB and standardized by subtracting the feature column’s mean and dividing by standard deviation over the entire data set. This same mean and standard deviation are also subtracted from the data during inference. The orientation values were normalized by the sensor fusion algorithm.

For the pressure dataset, we had two ground truth values per sample. The touch zone (0-6), with 0 representing no touch, and the 10-bit FSR value between 0-1023, with 15 used as a threshold for detecting pressure input. The distance dataset had three ground truth values per frame, each of the thumb-tip to sensor distances in meters.

**Table 1: BiRNN LSTM Pytorch hyperparameters for both pressure and distance models.**

Parameter	Value
Layers	3
Hidden Dimension	400
Dropout	0.2
Learning Rate	0.001
Batch Size	80
Sequence Length	40
Loss	SmoothL1
Optimization	AdamW

### 3.2 Neural Network Architecture

We based the machine learning architecture on established deep learning methods used with motion sequence IMU data [18, 46]. We developed a Bi-directional Recurrent Neural Network with Long Short-Term Memory cells (BiRNN LSTMs) as this was the highest

performing architecture in related work [18]. We created an identical model for each of our datasets using the Pytorch framework resulting in a *touch+pressure* and *distance* model. During hyperparameter search, we selected cell hidden dimension, number of layers, dropout, learning rate, batch size, sequence length, loss criterion and the optimization algorithm. The final hyperparameters for both models are in Table 1. Both models had regression outputs and used linear activation layers. We also regressed touch location linearly to simplify architecture, rounding touch location (0-6) to the nearest integer.

A Smooth L1 [13] was used as loss function of the optimization algorithm, which is a parametric Huber loss function. Huber loss uses L2 Mean Squared Error loss when the absolute element-wise error falls below beta (0.2); otherwise the L1 Mean Absolute Error Loss is used, making the system more robust to outliers in noisy IMU sensor data. An Adam with weight decay optimization algorithm [29] was used as well as an optimizer that reduces the learning rate when the loss improvement plateaus over successive training epochs, helping to improve loss-minima search efficiency.

### 3.3 Model Evaluation

The models were evaluated between training epochs using a split 0.8 to 0.2 training to evaluation set. We calculated accuracy of touch zone prediction in percent and pressure and distance errors as Mean Absolute Error from target across all training samples. Our best *touch+pressure* model resulted in 94.11% touch zone accuracy and 18.56 MAE for pressure. Our best *distance model* resulted in 0.41mm, 0.47 and 0.43mm MAE for distal, middle and proximal distance error respectively.

### 3.4 End-to-end Real-time Inference Pipeline

**3.4.1 Per-User real-time Calibration.** Users’ tactile sensitivity, and finger strength impact the amount of pressure they apply on their skin. The pipeline addresses this by normalizing the output pressure values, and removing output distance offsets. This results in a real-time per-user device calibration that *does not* modify the deep learning models or their inputs, but solely their output values. This calibration step happens before interacting by defining a minimal and maximal pressure level for each touch zone (values between 0 and 1024). Pressure values are then normalized and scaled to a percentage of this pressure interval.

The finger thickness of users affects the measurements of the hovering distances. MicroPress compensates with a one-time offset calibration users must perform before use. The 0mm hover distance offset is calibrated (i.e. the distance reported when the thumb and finger tip were touching) using a 0.2mm thick 3D printed jig held between the thumb and finger tip. The system then subtracts this offset value from future distance outputs.

As positioning depends on a precise magnetic field measurement, changes in sensor placement have a strong impact on the accuracy of the models. Since depth sensing relies mostly on Z-axis positioning, this error can be largely corrected using our calibration technique. However this remains a challenging issue due to the various hand morphologies that exist. In our study, we placed sensors rigorously in the middle of the participants finger phalanges in an effort to be as consistent as possible.

## 4 REAL-TIME INTERACTIVE SCENARIOS

In this section we present two interactive scenarios that demonstrate how users can leverage pressure and hover input in real-time. The first consists of a menu selection technique using pressure for targeting and hovering for validation. The second scenario consists of controlling the horizontal and vertical movements of a video game character in a 2D space with touch zones for directions and pressure for speed, and hover input for jumping. MicroPress supports low latency for comfort and accurate control in both scenarios.

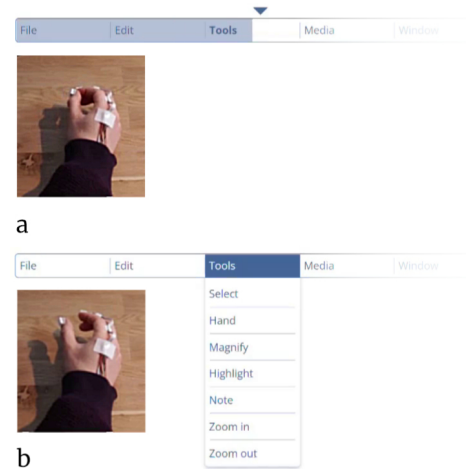


**Figure 3: Example of a pressure menu controlled with MicroPress. (a) The user targets a menu item using pressure, and dwells to select the item (indicated by the arrowhead). (b) They select the item by hovering beyond a threshold distance.**

### 4.1 Pressure Menu: Targeting and Selecting Commands in a List

This scenario presents a menu selection technique inspired from pressure targeting techniques [12, 38, 40] (see Video Figure at [01:40]). In this techniques the users perform pressure interactions on a single *touch zone*. They control a slider with *pressure* to target a menu item (light blue bar Figure 3a). They can *select* an item (i.e. a menu root or an item in a menu) by dwelling on a target for 1s to select it. A selected item is indicated by an arrowhead above (Figure 3a). The validation action consists of *hovering* above a threshold of 20mm for 1s (see Figure 3b) to confirm a selection. A menu item is deselected after a short delay if no pressure was detected. We used a Node.js server to communicate between MicroPress and the React application with data updated at 100 FPS.

This interaction technique is useful in controlling augmented reality devices such as smart glasses [19, 31] with subtle interactions when compared to mid-air gestures. One important challenge of targeting and selecting commands with pressure is the validation mechanism used [11]: *dwelling* and *quick release* mechanisms are prone to noisy input, while *instantaneous* validation commands require a dedicated command (e.g. a mouse button). The *select+validation* design allows users to select an item using pressure, then perform a validation action using hover.

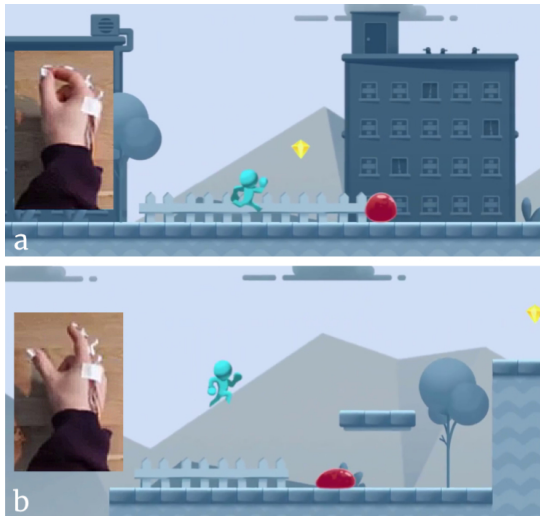


**Figure 4: Platform game: The user controls the character’s movement direction, speed and jump height respectively with touch zones, pressure (a) and hover input (b).**

## 4.2 Platform game: Controlling a Video Game Character’s Movement

In this scenario, the user controls a video game character in two dimensions (Figure 4, see Video Figure at [02:10]). The character moves horizontally at various speeds, and jumps at various heights. The user controls the direction of the lateral movements of the character by pressing two different *touch zones* (zone 4-MV and 6-DV). The level of *pressure* applied on each zone controls the movement speed of the character, with a running jump triggered at maximum pressure. *Hover input* controls the stationary jumping height with a linear function.

This example leverages embodied interactions for real-time gaming, thus providing a new type of playful user experience. Mapping pressure to motion here creates an interesting relationship as both the user and the character share a physical effort [33]. We used the Unity3D platform game template<sup>1</sup> and connected the player controls to the MicroPress pipeline. Data was updated at 100 FPS.

## 5 VALIDATION STUDY

We conducted a validation study to test the accuracy of MicroPress in real-time and to assess how the model generalizes to other hand geometries. We use a within-subject design that consists of two tasks: one to evaluate touch location and pressure accuracy, and the other to evaluate hover distance accuracy. This study has received approval from the ethics board of our university.

**5.0.1 Participants.** We recruited 8 right-handed volunteers from our university (4 identified as male, 4 identified as female) aged from 23 to 36 years old (median = 25.5) with various hand geometries to participate in the study. They did not participate in the training data collection. We measured their index finger and thumb dimensions for the distal, middle, and proximal segments. Measurements for the index finger segments were; 18 to 27mm ( $\bar{x} = 23.5$ , distal), 23 to 30mm ( $\bar{x} = 25.8$ , middle), and 31 to 45mm ( $\bar{x} = 37.0$ ,

<sup>1</sup><https://assetstore.unity.com/packages/templates/platformer-microgame-151055>

proximal) and for the thumb; 25 to 35mm ( $\bar{x} = 29.0$ , distal) and 30 to 40mm ( $\bar{x} = 33.6$ , proximal).

No participants reported any condition that could affect their ability to perform the study and there was no remuneration or reward for participating in the study.

For each task, participants began by sitting in front of a monitor with their hand flat on a marked position on the table in front of them, the sensing device powered off.

## 5.1 Task 1: Evaluating Pressure and Touch

**5.1.1 Experimental Variables.** We consider two independent variables for this first task. The *touch zone*: the distal, middle, and proximal phalanges for the volar (respectively DV, MV, PV) and the radial sides (respectively DR, MR, PR), see Figure 2a; and the *target pressure level*: 15, 30, 50, 70, and 85%.

**5.1.2 Task.** A web based user interface was designed following related work [25, 42]: the participant could control a slider moving up and down based on the pressure applied while wearing the sensor device (Figure 5a). Each trial indicated a touch location zone and pressure target. The participant would press on their index finger in the required touch zone and adjust the force to reach the target pressure level as accurately as possible. On their signal, the experimenter would start recording one second of touch and pressure data, similarly to dwell timing techniques used in the literature [4, 38]. Once recording was complete, the next trial would begin. We randomized touch location zone and pressure targets, with each combination repeated to give 6 touch zones x 5 pressure levels x 2 repetitions, or 60 trials per participant (overall  $60 \times 8 = 480$  trials). A session lasted around 40 minutes.

## 5.2 Task 2: Evaluating Hovering Distance

**5.2.1 Experimental Variables.** For the second task, we consider a unique independent variable: the *hover target distance*. The *target distance* consisted in 1, 2, 3, 4, 5, 6, 8, 10, 12, 14, 18 or 20mm, as well as a 0mm target that represents fingers touching between trials.

**5.2.2 Task.** The distance target was controlled using a 3D printed jig with 1mm steps, to precisely control the different distance measures between users (see Figure 5b). We used this technique to ensure a ground truth, as reaching a target distance between fingers is challenging. The participants held the correct distance on the jig using their thumb and finger tip, and the experimenter would record one second of data on their signal.

Similar to task 1, a web interface indicated the *target distance* and depicted a visual slider representing the distance between the thumb and the fingertip.

We randomized the distance targets, except for the 0mm targets between trials, and measured each target 2 times. Each participant performed (12 targets + 12 0mm reference targets) x 2 repetitions, or 48 trials which lasted around 20 minutes (overall,  $48 \times 8 = 384$  trials).

## 5.3 Results

We analyze the results using the Mean Absolute Error (MAE) metric. We report overall results per participant from both tasks in Table 2.

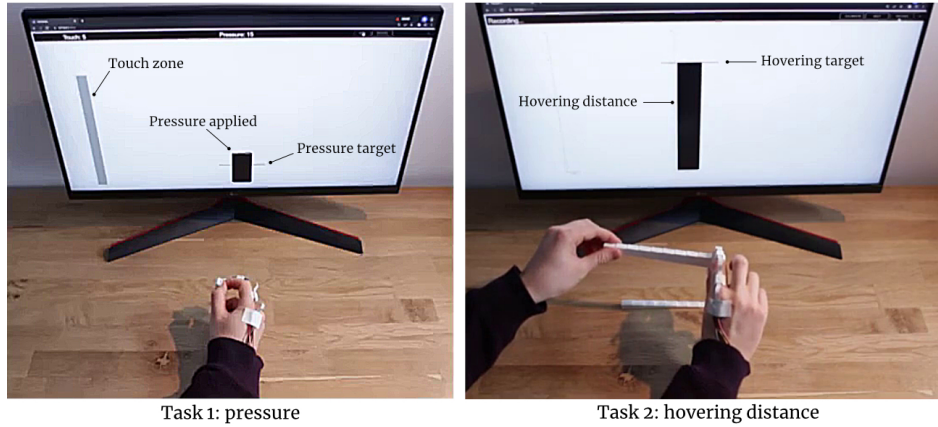


**Figure 5: Study setups for the two tasks. (a) The user controls a slider through pressure and must reach a given target. (b) The user controls a slider with hover distance and holds a given 3D printed jig reference distance.**

We removed outlying measurements from the dataset that represented mistakes in the trial task if their absolute error exceeded the overall mean plus 3 standard deviations (i.e.,  $\bar{x} + 3 \times \sigma$ ). We removed 60 outliers (1.83%) from task 1 data, and 10 (0.46%) from task 2 data.

**5.3.1 Pressure Absolute Error.** Overall, the system yielded low absolute errors based on the participants input (see Figure 6). We observe a mean absolute error of  $7.53 \pm 0.26$  between participants. While errors were very low for some of the participants (c.f., pressure error for participants 1 and 8 in Table 2), a Kruskal-Wallis test yielded significant differences between participants ( $\chi^2 = 351.7$ ,  $df = 7$ ,  $p < 0.001$ ), as represented on Figure 6.

A Kruskal-Wallis test comparing the pressure errors obtained for each touch zone revealed significant differences between them ( $\chi^2 = 29.89$ ,  $df = 5$ ,  $p < 0.001$ ). We observe the following errors:  $7.23 \pm 0.47\%$  (PR),  $6.74 \pm 0.47\%$  (PV),  $6.18 \pm 0.45\%$  (MR),  $7.78 \pm 0.55\%$  (MV),  $7.07 \pm 0.55\%$  (DR),  $5.28 \pm 0.30\%$  (DV).

**5.3.2 Hovering Distance Error.** Figure 6 depicts the mean absolute errors of the hovering distance for each distance target. On average, we observe an absolute error of  $0.57 \pm 0.04$ mm. A Kruskal-Wallis test revealed significant differences between distance targets ( $\chi^2 = 289.7$ ,  $df = 7$ ,  $p < 0.001$ ); the absolute error drops for distances larger than 1cm.

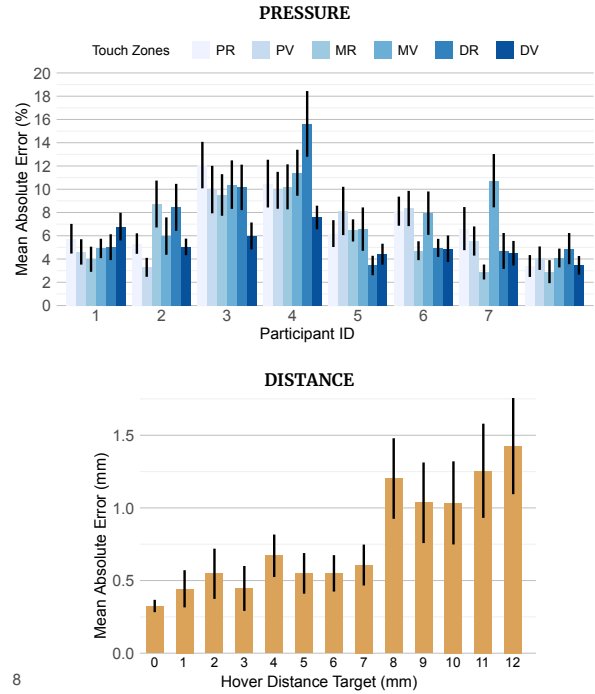


**Figure 6: Mean Absolute Error of pressure for all touch zones and hovering distances. Error bars depict 95% confidence intervals.**

**Table 2: Study results per participant. We report 95% confidence intervals for each measure.**

Participant	Task 1: Location and Pressure		Task 2: Hover Distance
	Location Accuracy (%)	Pressure MAE (%)	Distance MAE (mm)
1	87.3 ± 3.66	5.17 ± 0.45	1.06 ± 0.17
2	98.8 ± 1.04	6.13 ± 0.61	0.29 ± 0.08
3	94.0 ± 2.27	9.64 ± 0.76	0.08 ± 0.04
4	76.8 ± 4.06	10.8 ± 0.81	0.58 ± 0.13
5	97.9 ± 1.39	5.84 ± 0.56	0.49 ± 0.09
6	80.7 ± 3.79	6.48 ± 0.54	1.08 ± 0.12
7	85.6 ± 3.31	5.75 ± 0.64	0.60 ± 0.10
8	87.1 ± 3.21	3.79 ± 0.40	0.37 ± 0.09
Average	88.6 ± 1.09	6.71 ± 0.23	0.57 ± 0.04

## 6 DISCUSSION AND LIMITATIONS

While previous work proposed an extensive design space for thumb-to-finger interactions [41], it did not include interactions leveraging depth. MicroPress demonstrates that using a lightweight wearable device that does not obstruct the natural tactile feedback, one can sense pressure and hovering input in the context of thumb-to-finger interactions. We presented a validation study with eight participants to assess the efficacy of MicroPress. Results showed that the system yields high normalized pressure accuracy for various users at six distinct locations on their index finger ( $6.71 \pm 0.23\%$  absolute error), as well as high hovering distance accuracy ( $0.57 \pm 0.04$ mm



absolute error). These results demonstrate that *depth* for thumb-to-finger interactions is a dimension that can extend touch design spaces. Additionally, we presented two interactive scenarios posing challenges for real-time controls. They demonstrate how MicroPress can support real-time input in different contexts, and propose playful interactions and precise menu navigation and selection techniques. Our work focused on building a proof-of-concept device that enables pressure and hover input, but did not explore in depth all opportunities such input provide for thumb-to-finger interactions. Future work should explore this new space using knowledge gathered from studies on interaction techniques leveraging depth in the literature [9, 12, 15, 38].

MicroPress is only a proof-of-concept and comprises limitations that one needs to consider while building a similar device. The study results yielded strong variations between participants that are likely caused by the various hand geometries and the sensors placements. While collecting more data from more users or building more robust deep learning models might improve the device's accuracy, the placement of sensors on the hand remains a critical factor for ensuring consistency between training and real interaction contexts. We sought consistency while placing sensors in our study by placing each sensor at the middle of each phalanx, but this variable remains prone to slight offsets. We also did not fully control the users' hand movements while performing the set of tasks, but tried to reduce their possible impact by asking participants to perform movements with various hands rotation. We accounted for these types of problem using training data from users with different morphologies and randomly moving and rotating the hand while recording. While there is room for improvement, results obtained with models trained on few users data are very encouraging as they show the approach scales to various hand geometries without the need for a user-specific model.

The sets of users involved in training the models and to evaluating its efficiency remain small but diverse. We tried to balance this limitation by inviting participants with various hand geometries. The study aimed at validating the approach rather than testing its broad usability. While the results demonstrate the potential of our approach, they only provide limited evidence of the generalization. Further usability tests are required to understand how participants perceive the type of interactions performed and assess their efficiency. We hope our work can encourage extensive studies on depth input in the context of thumb-to-finger interactions.

We presented two real-time interactive applications demonstrating the MicroPress concept. These scenarios leverage one-handed depth input for selecting menu items and controlling a video game character in a 2D space. MicroPress interactions could also be leveraged for 3D mid-air interactions when combined with hand-pose algorithms used by conventional augmented- or virtual-reality devices such as the HoloLens or the Oculus Quest. They could complement most applications by enabling long-press and hover gestures conventionally used in mobile applications. They could also complement spatial interactions used to manipulate virtual objects in space like, for instance, the HoloLens finger-touching gesture for selecting virtual objects. MicroPress could enable to control the object parameters such as their size with pressure once the fingers touch.

The primary challenge of systems like MicroPress is to be able to run in ecological scenarios such as supporting interactions with an augmented reality system. Our technique depends on a magnetic field for precision, and optimizing its quality should be a focus for future work. Data driven models requires data that covers possible edge cases such as magnetically noisy environments, different sensor placements and hand geometries. An intrinsic property of magnetic field sensing is that their strength is inversely proportional with distance to the magnetic field source, the property that allows us to sense distance in our proof-of-concept. Due to this decrease in magnetic field strength however, the IMU's magnetometer is less sensitive to variations as distance increases. This reduces the IMU's Signal-to-Noise ratio adding uncertainty at larger distances. Our work did not control magnetic field interference, and we focused on a lab environment without shielding. The goal of this work was to provide a hardware proof-of-concept that demonstrates the benefits of the interaction technique. Future work should be aware of uncertainties faced in ecological scenarios and improve the device design in that regard.

While the system remains lightweight, it requires a desktop processing unit to provide an end-to-end real-time inference pipeline. We chose Bi-LSTM model in our prototype for its relevance and capabilities to detect time series of multi-dimensional data. Future data driven approaches would seek to optimize the model and frame rate so that it would be able to work with mobile or wearable devices. The models could also be unified to reduce computation overhead by training pressure and distance data with the same model. Finally, based on the desired interactive scenario, the number of sensors could be reduced. For instance, a ring based sensor or fingertip sensor would be effective at measuring pressure and hovering distance over a smaller finger area.

## 7 CONCLUSION

We presented MicroPress, a proof-of-concept system that can detect pressure and hovering input for thumb-to-finger interactions using a magnet coupled with IMUs and a deep learning pipeline. The location of the sensors allows to preserve the skin-to-skin natural tactile feedback of direct touch. While previous work addressing thumb-to-finger interactions only considered touch and swipe gestures, our work demonstrates one can sense depth in this context. We presented interactive scenarios demonstrating how controlling depth can enable embodied and subtle control. Finally, we validated the design of MicroPress with a study involving eight participants. The results show that the system yields low pressure and hover distance errors. These are promising results for depth control in the context of thumb-to-finger interactions leading the way for future work to explore this space more thoroughly.

## ACKNOWLEDGMENTS

This project received funding from the European Research Council (ERC StG Interactive Skin 714797). We would like to thank all the participants in our study and the people that reviewed this paper and helped us improve it.

## REFERENCES

- [1] Daniel Ashbrook, Patrick Baudisch, and Sean White. 2011. NENYA: Subtle and Eyes-Free Mobile Input with a Magnetically-Tracked Finger Ring (*CHI '11*). Association

- for Computing Machinery, New York, NY, USA, 2043–2046. <https://doi.org/10.1145/1978942.1979238>
- [2] Alberto Boem and Giovanni Maria Troiano. 2019. Non-Rigid HCI: A Review of Deformable Interfaces and Input. In *Proceedings of the 2019 on Designing Interactive Systems Conference* (San Diego, CA, USA) (DIS '19). Association for Computing Machinery, New York, NY, USA, 885–906. <https://doi.org/10.1145/3322276.3322347>
  - [3] Bosch. 2021. Sensor Fusion. <https://www.bosch-sensortec.com/software-tools/software/sensor-fusion-software/>.
  - [4] Jared Cechanowicz, Pourang Irani, and Sriram Subramanian. 2007. Augmenting the Mouse with Pressure Sensitive Input. In *Proceedings of the SIGCHI Conference on Human Factors in Computing Systems* (San Jose, California, USA) (CHI '07). ACM, New York, NY, USA, 1385–1394. <https://doi.org/10.1145/1240624.1240835>
  - [5] Liwei Chan, Yi-Ling Chen, Chi-Hao Hsieh, Rong-Hao Liang, and Bing-Yu Chen. 2015. CyclopsRing: Enabling Whole-Hand and Context-Aware Interactions Through a Fisheye Ring. In *Proceedings of the 28th Annual ACM Symposium on User Interface Software & Technology* (Charlotte, NC, USA) (UIST '15). Association for Computing Machinery, New York, NY, USA, 549–556. <https://doi.org/10.1145/2807442.2807450>
  - [6] Liwei Chan, Rong-Hao Liang, Ming-Chang Tsai, Kai-Yin Cheng, Chao-Huai Su, Mike Y. Chen, Wen-Huang Cheng, and Bing-Yu Chen. 2013. FingerPad: Private and Subtle Interaction Using Fingertips. In *Proceedings of the 26th Annual ACM Symposium on User Interface Software and Technology* (St. Andrews, Scotland, United Kingdom) (UIST '13). Association for Computing Machinery, New York, NY, USA, 255–260. <https://doi.org/10.1145/2501988.2502016>
  - [7] Ke-Yu Chen, Kent Lyons, Sean White, and Shwetak Patel. 2013. UTrack: 3D Input Using Two Magnetic Sensors (UIST '13). Association for Computing Machinery, New York, NY, USA, 237–244. <https://doi.org/10.1145/2501988.2502035>
  - [8] Ke-Yu Chen, Shwetak N. Patel, and Sean Keller. 2016. Finexus: Tracking Precise Motions of Multiple Fingertips Using Magnetic Sensing. In *Proceedings of the 2016 CHI Conference on Human Factors in Computing Systems* (San Jose, California, USA) (CHI '16). Association for Computing Machinery, New York, NY, USA, 1504–1514. <https://doi.org/10.1145/2858036.2858125>
  - [9] Victor Cheung, Jens Heydekorn, Stacey Scott, and Raimund Dachselt. 2012. Re-visiting hovering: interaction guides for interactive surfaces. In *Proceedings of the 2012 ACM international conference on Interactive tabletops and surfaces*, 355–358.
  - [10] Christian Corsten, Bjoern Daehlmann, Simon Voelker, and Jan Borchers. 2017. BackXPRESS: Using Back-of-Device Finger Pressure to Augment Touchscreen Input on Smartphones. In *Proceedings of the 2017 CHI Conference on Human Factors in Computing Systems* (Denver, Colorado, USA) (CHI '17). Association for Computing Machinery, New York, NY, USA, 4654–4666. <https://doi.org/10.1145/3025453.3025565>
  - [11] Christian Corsten, Simon Voelker, and Jan Borchers. 2017. Release, Don't Wait! Reliable Force Input Confirmation with Quick Release. In *Proceedings of the 2017 ACM International Conference on Interactive Surfaces and Spaces* (Brighton, United Kingdom) (ISS '17). Association for Computing Machinery, New York, NY, USA, 246–251. <https://doi.org/10.1145/3132272.3134116>
  - [12] Bruno Fruchard, Paul Strohmeier, Roland Bennewitz, and Jürgen Steimle. 2021. Squish This: Force Input on Soft Surfaces for Visual Targeting Tasks. In *Proceedings of the 2021 CHI Conference on Human Factors in Computing Systems* (Yokohama, Japan) (CHI '21). Association for Computing Machinery, New York, NY, USA, Article 219, 9 pages. <https://doi.org/10.1145/3411764.3445623>
  - [13] Ross B. Girshick. 2015. Fast R-CNN. CoRR abs/1504.08083 (2015). arXiv:1504.08083 <http://arxiv.org/abs/1504.08083>
  - [14] Jun Gong, Yang Zhang, Xia Zhou, and Xing-Dong Yang. 2017. Pyro: Thumb-Tip Gesture Recognition Using Pyroelectric Infrared Sensing. In *Proceedings of the 30th Annual ACM Symposium on User Interface Software and Technology* (Québec City, QC, Canada) (UIST '17). Association for Computing Machinery, New York, NY, USA, 553–563. <https://doi.org/10.1145/3126594.3126615>
  - [15] Ken Hinckley, Seongkook Heo, Michel Pahud, Christian Holz, Hrvoje Benko, Abigail Sellen, Richard Banks, Kenton O'Hara, Gavin Smyth, and William Buxton. 2016. Pre-Touch Sensing for Mobile Interaction. In *Proceedings of the 2016 CHI Conference on Human Factors in Computing Systems* (San Jose, California, USA) (CHI '16). Association for Computing Machinery, New York, NY, USA, 2869–2881. <https://doi.org/10.1145/2858036.2858095>
  - [16] <https://github.com/aster94>. 2021. Sensorfusion 1.0.3. <https://www.arduino.cc/reference/en/libraries/sensorfusion/>.
  - [17] Da-Yuan Huang, Liwei Chan, Shuo Yang, Fan Wang, Rong-Hao Liang, De-Nian Yang, Yi-Ping Hung, and Bing-Yu Chen. 2016. DigitSpace: Designing Thumb-to-Fingers Touch Interfaces for One-Handed and Eyes-Free Interactions (CHI '16). Association for Computing Machinery, New York, NY, USA, 1526–1537. <https://doi.org/10.1145/2858036.2858483>
  - [18] Yinghao Huang, Manuel Kaufmann, Emre Aksan, Michael J. Black, Otmar Hilliges, and Gerard Pons-Moll. 2018. Deep Inertial Poser: Learning to Reconstruct Human Pose from Sparse Inertial Measurements in Real Time. *ACM Trans. Graph.* 37, 6, Article 185 (Dec. 2018), 15 pages. <https://doi.org/10.1145/3272127.3275108>
  - [19] Snap Inc. 2022. Spectacles. <https://www.spectacles.com/fr/>.
  - [20] Yu Ishikawa, Buntarou Shizuki, and Junichi Hoshino. 2017. Evaluation of Finger Position Estimation with a Small Ranging Sensor Array. In *Proceedings of the 5th Symposium on Spatial User Interaction* (Brighton, United Kingdom) (SUI '17). Association for Computing Machinery, New York, NY, USA, 120–127. <https://doi.org/10.1145/3131277.3132176>
  - [21] Keiko Katsuragawa, Ju Wang, Ziyang Shan, Ningshan Ouyang, Omid Abari, and Daniel Vogel. 2019. Tip-Tap: Battery-Free Discrete 2D Fingertip Input. In *Proceedings of the 32nd Annual ACM Symposium on User Interface Software and Technology* (New Orleans, LA, USA) (UIST '19). Association for Computing Machinery, New York, NY, USA, 1045–1057. <https://doi.org/10.1145/3332165.3347907>
  - [22] Minwoo Kim, Jaechan Cho, Seongjoo Lee, and Yunho Jung. 2019. IMU Sensor-Based Hand Gesture Recognition for Human-Machine Interfaces. *Sensors* 19, 18 (2019). <https://doi.org/10.3390/s19183827>
  - [23] Kenneth Lai and Svetlana N Yanushkevich. 2018. CNN+ RNN depth and skeleton based dynamic hand gesture recognition. In *2018 24th International Conference on Pattern Recognition (ICPR)*. IEEE, 3451–3456.
  - [24] Matthew Lakier, Dimcho Karakashev, Yixin Wang, and Ian Goldberg. 2020. Augmented Unlocking Techniques for Smartphones Using Pre-Touch Information. In *Symposium on Spatial User Interaction* (Virtual Event, Canada) (SUI '20). Association for Computing Machinery, New York, NY, USA, Article 17, 5 pages. <https://doi.org/10.1145/3385959.3418455>
  - [25] Ke Li, Raviraj Nataraj, Tamara L. Marquardt, and Zong-Ming Li. 2013. Directional Coordination of Thumb and Finger Forces during Precision Pinch. *PLOS ONE* 8, 11 (11 2013), 1–8. <https://doi.org/10.1371/journal.pone.0079400>
  - [26] Z. Li, Z. Lei, A. Yan, E. Solovey, and K. Pahlavan. 2020. ThuMouse: A Micro-gesture Cursor Input through mmWave Radar-based Interaction. In *2020 IEEE International Conference on Consumer Electronics (ICCE)*, 1–9. <https://doi.org/10.1109/ICCE46568.2020.9043082>
  - [27] Jaime Lien, Nicholas Gillian, M. Emre Karagozler, Patrick Amihood, Carsten Schwesig, Erik Olson, Hakim Raja, and Ivan Poupyrev. 2016. Soli: Ubiquitous Gesture Sensing with Millimeter Wave Radar. *ACM Trans. Graph.* 35, 4, Article 142 (July 2016), 19 pages. <https://doi.org/10.1145/2897824.2925953>
  - [28] Christian Loclair, Sean Gustafson, and Patrick Baudisch. 2010. PinchWatch: a wearable device for one-handed microinteractions. In *Proc. MobileHCI*, Vol. 10. Citeseer.
  - [29] Ilya Loshchilov and Frank Hutter. 2019. Decoupled Weight Decay Regularization. arXiv:1711.05101 [cs.LG]
  - [30] Jess McIntosh, Paul Strohmeier, Jarrod Knibbe, Sebastian Boring, and Kasper Hornbæk. 2019. Magnetips: Combining Fingertip Tracking and Haptic Feedback for Around-Device Interaction. In *Proceedings of the 2019 CHI Conference on Human Factors in Computing Systems* (Glasgow, Scotland UK) (CHI '19). Association for Computing Machinery, New York, NY, USA, 1–12. <https://doi.org/10.1145/3290605.3300638>
  - [31] Microsoft. 2022. Hololens. <https://www.microsoft.com/en-us/hololens>.
  - [32] Franziska Mueller, Dushyant Mehta, Oleksandr Softnychenko, Srinath Sridhar, Dan Casas, and Christian Theobalt. 2017. Real-Time Hand Tracking Under Occlusion From an Egocentric RGB-D Sensor. In *Proceedings of the IEEE International Conference on Computer Vision (ICCV)*.
  - [33] Florian 'Floyd' Mueller, Richard Byrne, Josh Andres, and Rakesh Patibanda. 2018. *Experiencing the Body as Play*. Association for Computing Machinery, New York, NY, USA, 1–13. <https://doi.org/10.1145/3173574.3173784>
  - [34] Aditya Shekhar Nittala, Anusha Withana, Narjes Pourjafarian, and Jürgen Steimle. 2018. Multi-touch skin: A thin and flexible multi-touch sensor for on-skin input. In *Proceedings of the 2018 CHI Conference on Human Factors in Computing Systems*, 1–12.
  - [35] Keunwoo Park, Sunbum Kim, Youngwoo Yoon, Tae-Kyun Kim, and Geehyuk Lee. 2020. DeepFisheye: Near-Surface Multi-Finger Tracking Technology Using Fisheye Camera. In *Proceedings of the 33rd Annual ACM Symposium on User Interface Software and Technology* (Virtual Event, USA) (UIST '20). Association for Computing Machinery, New York, NY, USA, 1132–1146. <https://doi.org/10.1145/3379337.3415818>
  - [36] Adam Paszke, Sam Gross, Francisco Massa, Adam Lerer, James Bradbury, Gregory Chanan, Trevor Killeen, Zeming Lin, Natalia Gimelshein, Luca Antiga, Alban Desmaison, Andreas Kopf, Edward Yang, Zachary DeVito, Martin Raison, Alykhan Tejani, Sasank Chilamkurthy, Benoit Steiner, Lu Fang, Junjie Bai, and Soumith Chintala. 2019. PyTorch: An Imperative Style, High-Performance Deep Learning Library. In *Advances in Neural Information Processing Systems 32*. Curran Associates, Inc., 8024–8035. <http://papers.neurips.cc/paper/9015-pytorch-an-imperative-style-high-performance-deep-learning-library.pdf>
  - [37] F. H. Raab, E. B. Blood, T. O. Steiner, and H. R. Jones. 1979. Magnetic Position and Orientation Tracking System. *IEEE Trans. Aerospace Electron. Systems* AES-15, 5 (1979), 709–718. <https://doi.org/10.1109/TAES.1979.308860>
  - [38] Gonzalo Ramos, Matthew Boulos, and Ravin Balakrishnan. 2004. Pressure Widgets. In *Proceedings of the SIGCHI Conference on Human Factors in Computing Systems* (Vienna, Austria) (CHI '04). ACM, New York, NY, USA, 487–494. <https://doi.org/10.1145/985692.985754>

- [39] Christina Salchow-Hömmen, Leonie Callies, Daniel Laidig, Markus Valtin, Thomas Schauer, and Thomas Seel. 2019. A Tangible Solution for Hand Motion Tracking in Clinical Applications. *Sensors* 19, 1. <https://doi.org/10.3390/s19010208>
- [40] Kang Shi, Pourang Irani, Sean Gustafson, and Sriram Subramanian. 2008. PressureFish: A Method to Improve Control of Discrete Pressure-based Input. In *Proceedings of the SIGCHI Conference on Human Factors in Computing Systems* (Florence, Italy) (*CHI '08*). ACM, New York, NY, USA, 1295–1298. <https://doi.org/10.1145/1357054.1357256>
- [41] Mohamed Soliman, Franziska Mueller, Lena Hegemann, Joan Sol Roo, Christian Theobalt, and Jürgen Steimle. 2018. FingerInput: Capturing Expressive Single-Hand Thumb-to-Finger Microgestures. In *Proceedings of the 2018 ACM International Conference on Interactive Surfaces and Spaces* (Tokyo, Japan) (*ISS '18*). Association for Computing Machinery, New York, NY, USA, 177–187. <https://doi.org/10.1145/3279778.3279799>
- [42] Paul Strohmeier, Jarrod Knibbe, Sebastian Boring, and Kasper Hornbæk. 2018. ZPatch: Hybrid Resistive/Capacitive ETextile Input. In *Proceedings of the Twelfth International Conference on Tangible, Embedded, and Embodied Interaction* (Stockholm, Sweden) (*TEI '18*). Association for Computing Machinery, New York, NY, USA, 188–198. <https://doi.org/10.1145/3173225.3173242>
- [43] Hsin-Ruey Tsai, Cheng-Yuan Wu, Lee-Ting Huang, and Yi-Ping Hung. 2016. ThumbRing: Private Interactions Using One-Handed Thumb Motion Input on Finger Segments. In *Proceedings of the 18th International Conference on Human-Computer Interaction with Mobile Devices and Services Adjunct* (Florence, Italy) (*MobileHCI '16*). Association for Computing Machinery, New York, NY, USA, 791–798. <https://doi.org/10.1145/2957265.2961859>
- [44] Roel Vertegaal and Ivan Poupyrev. 2008. Organic user interfaces. *Commun. ACM* 51, 6 (2008), 26–30.
- [45] Nicolas Villar, Daniel Cletheroe, Greg Saul, Christian Holz, Tim Regan, Oscar Salandin, Misha Sra, Hui-Shyong Yeo, William Field, and Haiyan Zhang. 2018. Project Zanzibar: A Portable and Flexible Tangible Interaction Platform. In *Proceedings of the 2018 CHI Conference on Human Factors in Computing Systems* (Montreal QC, Canada) (*CHI '18*). Association for Computing Machinery, New York, NY, USA, 1–13. <https://doi.org/10.1145/3173574.3174089>
- [46] Saiwen Wang, Jie Song, Jaime Lien, Ivan Poupyrev, and Otmar Hilliges. 2016. Interacting with Soli: Exploring Fine-Grained Dynamic Gesture Recognition in the Radio-Frequency Spectrum. In *Proceedings of the 29th Annual Symposium on User Interface Software and Technology* (Tokyo, Japan) (*UIST '16*). Association for Computing Machinery, New York, NY, USA, 851–860. <https://doi.org/10.1145/2984511.2984565>
- [47] Martin Weigel, Vikram Mehta, and Jürgen Steimle. 2014. More than Touch: Understanding How People Use Skin as an Input Surface for Mobile Computing. In *Proceedings of the SIGCHI Conference on Human Factors in Computing Systems* (Toronto, Ontario, Canada) (*CHI '14*). Association for Computing Machinery, New York, NY, USA, 179–188. <https://doi.org/10.1145/2556288.2557239>
- [48] Martin Weigel, Aditya Shekhar Nittala, Alex Olwal, and Jürgen Steimle. 2017. Skinmarks: Enabling interactions on body landmarks using conformal skin electronics. In *Proceedings of the 2017 CHI Conference on Human Factors in Computing Systems*. 3095–3105.
- [49] Eric Whitmire, Mohit Jain, Divye Jain, Greg Nelson, Ravi Karkar, Shwetak Patel, and Mayank Goel. 2017. DigiTouch: Reconfigurable Thumb-to-Finger Input and Text Entry on Head-Mounted Displays. *Proc. ACM Interact. Mob. Wearable Ubiquitous Technol.* 1, 3, Article 113 (Sept. 2017), 21 pages. <https://doi.org/10.1145/3130978>
- [50] Graham Wilson, Craig Stewart, and Stephen A. Brewster. 2010. Pressure-based Menu Selection for Mobile Devices. In *Proceedings of the 12th International Conference on Human Computer Interaction with Mobile Devices and Services* (Lisbon, Portugal) (*MobileHCI '10*). ACM, New York, NY, USA, 181–190. <https://doi.org/10.1145/1851600.1851631>
- [51] Zheer Xu, Pui Chung Wong, Jun Gong, Te-Yen Wu, Aditya Shekhar Nittala, Xiaojun Bi, Jürgen Steimle, Hongbo Fu, Kening Zhu, and Xing-Dong Yang. 2019. TipText: Eyes-Free Text Entry on a Fingertip Keyboard. In *Proceedings of the 32nd Annual ACM Symposium on User Interface Software and Technology* (New Orleans, LA, USA) (*UIST '19*). Association for Computing Machinery, New York, NY, USA, 883–899. <https://doi.org/10.1145/3332165.3347865>
- [52] Hui-Shyong Yeo, Erwin Wu, Juyoung Lee, Aaron Quigley, and Hideki Koike. 2019. Opisthenar: Hand Poses and Finger Tapping Recognition by Observing Back of Hand Using Embedded Wrist Camera. In *Proceedings of the 32nd Annual ACM Symposium on User Interface Software and Technology* (New Orleans, LA, USA) (*UIST '19*). Association for Computing Machinery, New York, NY, USA, 963–971. <https://doi.org/10.1145/3332165.3347867>
- [53] Shumin Zhai, Paul Milgram, and William Buxton. 1996. The Influence of Muscle Groups on Performance of Multiple Degree-of-Freedom Input. In *Proceedings of the SIGCHI Conference on Human Factors in Computing Systems* (Vancouver, British Columbia, Canada) (*CHI '96*). Association for Computing Machinery, New York, NY, USA, 308–315. <https://doi.org/10.1145/238386.238534>
- [54] Yang Zhang and Chris Harrison. 2015. Tomo: Wearable, Low-Cost Electrical Impedance Tomography for Hand Gesture Recognition. In *Proceedings of the 28th Annual ACM Symposium on User Interface Software & Technology* (Charlotte, NC, USA) (*UIST '15*). Association for Computing Machinery, New York, NY, USA, 167–173. <https://doi.org/10.1145/2807442.2807480>
- [55] Junhan Zhou, Yang Zhang, Gierad Laput, and Chris Harrison. 2016. AuraSense: Enabling Expressive Around-Smartwatch Interactions with Electric Field Sensing. In *Proceedings of the 29th Annual Symposium on User Interface Software and Technology* (Tokyo, Japan) (*UIST '16*). Association for Computing Machinery, New York, NY, USA, 81–86. <https://doi.org/10.1145/2984511.2984568>